New Implementation of the Moment Method Based on the Impedance Operator to Study the Dispersion Characteristics of Microstrip Lines

Nejla OUESLATI[1] and Taoufik AGUILI[1]

[1]SysCom Laboratory, National Engineering School,
B.P 37 Le belvedere 1002 Tunis,
Tunisia

Abstract

An original integral method (MR-GEC) based on the moment method (MoM) is developed in this paper to study dispersion characteristics of uniform microstrip lines. The introduction of a novel impedance operator by using the Generalized Equivalent Circuit (GEC) approach offers the simplicity of the resolution of the boundary problems by the transposition of problems in fields to electric circuit problems and the implementation of numerical procedures with a minimum of analytical pretreatment. The impedance/admittance operator is discretized in matrix forms by Galerkin's procedure, using orthonormal periodic wavelets as testing functions. A new algorithm is developed employing a multiresolution analysis (MR) which is based on the Discrete Wavelet Transform (DWT) to reduce the computational effort in filling the impedance matrix entries. Using the proposed MR-GEC method and subsequently applying a threshold operation, a substantial reduction in the number of elements of the impedance matrix and in the memory storage are attained without virtually affecting the solution accuracy. The numerical results obtained in this paper reveal the validity of the proposed method.

Keywords: *moment method (MoM), Generalized Equivalent Circuit approach (GEC, wavelet, impedance operator, boundary conditions.*

1. Introduction

Microstrip lines have been of fundamental importance for the development of microwave integrated circuits [1- 2-3]. A number of workers have been studied the dispersion properties of microstrip lines on isotropic dielectric substrates [4]: Mittra and Itoh [5-6-7-8], Krage and Haddad [24]. All the publications in this domain [10-11] have shown that the integral formulation, specifically the moment method, was the best to set the full wave methods more efficiently. The method of moments uses the integral from of Maxwell's equations. These equations are solved by the finite linear space approximation which leads to a matrix equation of which the rank is proportional to the number of unknowns. However, in most cases, knowledge of the Green' functions, either in simple functional form or series expansion form, are required. This limits the use of MoM to simple structures in which Green's functions are available.

The integral equation needs enormous amount of analytical effort to implement when supports of basis and testing functions are overlapping or share some common points. Indeed, the application of the MoM gives rise to singular integrals that causes problems in the compute of matrix elements since, it is necessary to extract the singularity rendering the technique quite time consuming.

On the other hand, different formulation are needed when the structure changes. Indeed, the application of the spatial-domain MOM requires the necessary Green's functions in the spatial domain that can be obtained from their spectral domain counterparts, therefor, additional numerical implementation are needed.

In this paper, we introduce a new formulation using a Surface Impedance Operator for bypassing conventional surface integral equations limitations and to circumventing the MoM difficulties by combining the Generalized Equivalent Circuit (GEC) to the Moment Method (MoM) [6, 7]. The contribution of this method lies in the simplicity of transposition problems in fields to electric circuit problems and the possibility of elaboration of numerical procedures rotatable on PC with a minimum of analytical pretreatment. In this formulation, the impedance operator is used instead of the integro-differential operator [8] simplifying then the transition between spectral and spatial domains. This operator can translate the boundary conditions of the studied problem through the equivalent circuit and the integral equations are obtained by simple application of Ohm's and Kirchhoff's laws.

To increase the efficiency of the new formulation of the MoM, the use of wavelet as trial functions is proposed. The application of the discrete wavelet transform (DWT) allows the reduction of the computation time. It is also shown that the use of wavelets bases allows an efficient sparsification of the matrix, which permits a significant reduction of the central processing unit time and the

memory storage. The developed method has been applied to solve electromagnetic equation for a uniform microstrip line located in the cross section of a rectangular waveguide.
Easily implementable in commercial simulators and successfully applied to planar lines on iso/anisotropic truncated substrates [13, 14], this technique consists to adequately formulate the boundary conditions by considering the fictitious propagation in the transverse direction of the line.

2. Formulation of the MR-GEC

The proposed full-wave approach uses the Galerkin's procedure to obtain a homogeneous system of algebraic equations from which the propagation constant β or the effective permittivity ε_{eff} for uniform microstrip line.

2.1 Studied structure

The structure designed to highlight the contribution of the GEC approach to alleviate the complexity of the MoM in modeling structures through the use of the impedance operator instead the green functions is already studied by CJ RAILTON and T. ROZZI in [19]. The dielectric substrate used to analyze shielded microstrip line is assumed to be homogeneous, isotropic, and lossless with high permittivity $\varepsilon_r = 8.875$ and a height of $h = 1.27\ mm$. Its upper face is partially metalized by one parallel uniform zero-thickness and perfectly conducting strip where (oz) axis is chosen to be the direction of wave propagation, the width of the strip is $w = 1.27\ mm$ as shown in (Fig. 1). We choose to enclose the considered structure by EEEE boundary conditions: four perfect electric boundaries to the top, the bottom and two lateral boundaries.

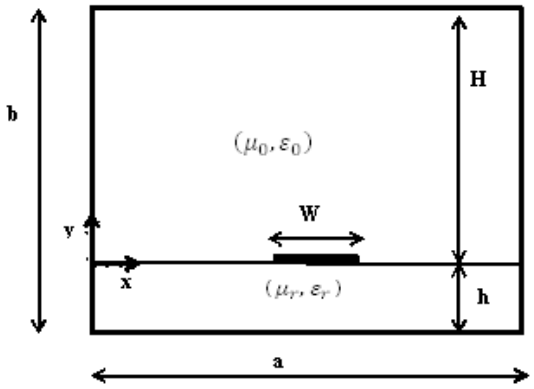

Fig. 1 Cross section of a shielded microstrip line: a=12.7 mm, b=12.7 mm, h=1.27 mm, $\varepsilon_r = 8.875$, W=1.27 mm.

2.2 Structure modeling

The studied problem is modeled using the GEC method [5] which translates the boundary conditions and the relations between electric and magnetic fields into an equivalent circuit, as shown in Fig. 2.
The boundary conditions of magnetic field are translated in this representation by the Kirchhoff law applied to the electric field [6].
The equations of the problem are obtained by writing that the trial functions are "'virtual" (i.e. the complex power which go through these sources is zero).This rule has been widely used in the problems of waveguides by the Spectral Domain Approach.
The relation between the electric field and the current is identified using the impedance operator. In fact, when we apply the laws of tension and current, we deduce the relation between virtual and real sources and its duals.

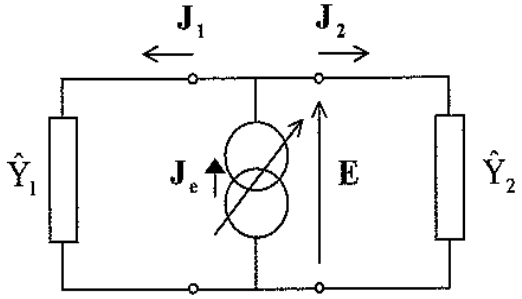

Fig. 2 Equivalent circuit of the uniform shielded microstrip line.

Based on the implementing rules, we can formulate the problem of searching the dispersion curves of the structure by studying its equivalent circuit. To do this, we bring back the different modes propagating in space on the study area and we transpose the top cover of the box to a dipole representing the admittance of vacuum $\hat{Y}_1$. The same applies to the ground plane which is replaced by a dipole representative of the admittance shorted $\hat{Y}_2$.
The equivalent circuit of the transverse section of unilateral microstrip line with negligible thickness includes the presence of a nonzero virtual source represented by the transverse surface current density $\vec{J}_e$ on the conducting strip, $\vec{E}$ its dual. It can be expressed in terms of the magnetic fields defined in this discontinuity plane as:

$$\vec{J}_M = \vec{H}^1 \wedge \vec{n}^1 + \vec{H}^2 \wedge \vec{n}^2 = \vec{J}_1 + \vec{J}_2 \qquad (1)$$

Where $\vec{n}^1$ and $\vec{n}^2$ indicate unit vectors normal to the discontinuity plane and directed toward $y > 0$ and $y < 0$, respectively.
So $\vec{J}_e$ is expressed as a series of known test functions weighted by unknown coefficients.

Based on its corresponding equivalent circuit model depicted in Fig. 2, the generalized Ohm and Kirchhoff laws are then rewritten as equations system:

$$\begin{cases} E = \hat{Y}_2^{-1} J_2 \\ E = \hat{Y}_1^{-1} J_1 \\ J_1 + J_2 = Je \end{cases} \quad (2)$$

We obtain then the following system:

$$\begin{cases} J_e = J_1 + J_2 = J \\ E = (\hat{Y}_1 + \hat{Y}_2)^{-1} J_e = \hat{Z} J_e \end{cases} \quad (3)$$

A formal relation between sources (real and virtual) and their duals is given as:

$$\begin{pmatrix} J \\ E \end{pmatrix} = \begin{pmatrix} 0 & 1 \\ 0 & \hat{Z} \end{pmatrix} \begin{pmatrix} 0 \\ J_e \end{pmatrix} \quad (4)$$

Note that the above equations have been set without any assumption or restriction. In fact, as demonstrated in [23], the spectral representation of the admittance operator leads to a diagonal admittance matrix. Consequently, the impedance operator always exists, with $\hat{Z} = \hat{Y}^{-1}$. They are discrete operators applied on the spectral domain. Each one can also be called a spatial-spectral operator and it allows transition from spectral to spatial domain.

The matrix representation of $\hat{Z}$ or $\hat{Y}$operators should be determined to obtain the overall matrix via the Galerkin's technique.

The first step in the computation process is evaluation of the term $\hat{Z}J_e$. Some transformations are needed in order to compute this term.

The impedance operator used here, who is an alternative of the Green operator in the spectral field, is described using modal basis of the guide. It represents the reaction of the environment and describes the contribution of the localized modes.

This method requires the involvement of a complete set of orthogonal basis functions $\{|f_n\rangle\}_{n=0,N}$, with N the number of modes), which should satisfy the boundary conditions imposed by the shielding [23]. The basis functions are described as:

$$f_n^{TE} \begin{cases} f_{nx}^{TE}(x) = \sqrt{\frac{\tau_n}{a}} \frac{-\gamma_z}{\sqrt{\left(\frac{n\pi}{a}\right)^2 + |\gamma_z|^2}} \cos\left(\frac{n\pi}{a}x\right) \\ f_{nz}^{TE}(x) = \sqrt{\frac{\tau_n}{a}} \frac{\frac{n\pi}{a}}{\sqrt{\left(\frac{n\pi}{a}\right)^2 + |\gamma_z|^2}} \sin\left(\frac{n\pi}{a}x\right) \end{cases} \quad (5)$$

$$f_n^{TM} \begin{cases} f_{nx}^{TM}(x) = \sqrt{\frac{\tau_n}{a}} \frac{\frac{n\pi}{a}}{\sqrt{\left(\frac{n\pi}{a}\right)^2 + |\gamma_z|^2}} \cos\left(\frac{n\pi}{a}x\right) \\ f_{nz}^{TM}(x) = \sqrt{\frac{\tau_n}{a}} \frac{-\gamma_z}{\sqrt{\left(\frac{n\pi}{a}\right)^2 + |\gamma_z|^2}} \sin\left(\frac{n\pi}{a}x\right) \end{cases} \quad (6)$$

where $\tau_n = \begin{cases} 1; n = 0 \\ 2; n \neq 0 \end{cases}$

The modal basis is orthogonal in terms of the scalar product if the propagation constant in the direction (oz) is imaginary. It is defined as a function of the wave-number β as:

$$\gamma_z = j\beta \quad (7)$$

By solving Maxwell's equations to calculate the electric field components in the transverse plane, we define the parameters necessary for the implementation of our simplified version of the MoM which is based on the impedance operator.

We thus define the propagation constant of the transverse modes by:

$$p_{ni}^2 = \left(\frac{n\pi}{a}\right)^2 - \gamma_z^2 - k_0^2 i \quad (8)$$

where $i = \begin{cases} 1; vacuum \\ \varepsilon_r; dielectric \end{cases}$

The admittances of the TE and TM modes on either side of the line are defined by:

$$y_{ni}^{TE} = \frac{p_{ni}}{j\omega\mu_0} \quad (9)$$

$$y_{ni}^{TM} = \frac{j\omega\varepsilon_0 i}{p_{ni}}$$

The input impedances looking into the equivalent circuit at $y = 0$ are given by:

$$z_n^{TE} = \frac{1}{Y_{nh}^{TE} + Y_{nH}^{TE}}$$
$$z_n^{TM} = \frac{1}{Y_{nh}^{TM} + Y_{nH}^{TM}} \quad (10)$$

where

$$Y_{ni}^{TE} = y_{ni}^{TE} \coth(p_{ni} \times dis\tan ce)$$
$$Y_{ni}^{TM} = y_{ni}^{TM} \coth(p_{ni} \times dis\tan ce)$$

$$dis\tan ce = \begin{cases} h; i = dielectrc \\ H; i = vacuum \end{cases}$$

are the admittances seen by each mode at the interface of the strip.
The expression of the impedance operator is expressed as:

$$\hat{Z} = \sum_{n=0} \left| f_n^{TE} \right\rangle z_n^{TE} \left\langle f_n^{TE} \right| + \sum_{n=1} \left| f_n^{TM} \right\rangle z_n^{TM} \left\langle f_n^{TM} \right| \quad (11)$$

In the above equation, $|f_n\rangle \langle f_n|$ represents the projection operator on the basis vectors $\{|f_n\rangle\}_{n=0,N}$ while "$\langle\,|$ and $|\,\rangle$" represent the ''bra'' and ''ket'' operators, respectively. Note that the product of vector ''bra'' $\langle f_n|$ with vector ''ket'' $|f_{n'}\rangle$ represents the inner product of these two quantities deducted from the integral calculation through the integration domain ID such as $\int \vec{f}(r)^{*t} \vec{g}(r) dr$.
We use the Galerkin method to solve the Equation 8 numerically. The method consists in determining the system matrix from the equivalent circuit, and make projections based on trial functions.

2.3 Choice of trial functions: wavelet expansion

An adequate choice of trial functions is essential to assure a reliable solution with minimum numerical treatments and processing time. Indeed, a suitable choice of trial functions leads to a better configuration of the transverse current density on the metal of the transmission line. This choice must respect several convergence criteria [15] as detailed in [17].

In this article, the trial functions are presented as a superposition of wavelets at several scales including the scaling function. A Galerkin method is then applied, where the set of trial functions are used as weighting functions. The wavelets used here are Haar basis an orthogonal type. Its study is useful from theoretical point of view, because it offers an intuitive understanding of many multi-resolution properties. Furthermore, due to its simplicity Haar wavelets are widely employed.
The wavelets are applied directly upon the integral equation. J_e will be represented as a linear combination of the set wavelets functions and scaling functions as follow [20-21]:

$$J_e(x) = \sum_{k=0}^{2^{s(-)}} c_{s(-),k} \phi_{s(-),k}(x) + \sum_{s=s(-)}^{s(+)} \sum_{k=0}^{2^s-1} d_{s,k} \psi_{s,k}(x) \quad (12)$$

Where *s(-)* is the coarsest resolution level, *s(+)* is the finest resolution level and *k* is the translation index [22].
The fact that the wavelets are orthogonal and the presence of vanishing moment, this is enabling sparse matrix production.
The electric field has to be zero on the metallized strips, thus it could be written:

$$|E\rangle^{(TE+TM)} = (\hat{Z}|J\rangle)^{(TE+TM)} = |0\rangle \ (on\ the\ metal) \quad (13)$$

When applying Galerkin procedure to (8), we obtain the set of matrix equation as follow:

$$\begin{bmatrix} [Z_{\phi\phi}] & [Z_{\phi\psi}] \\ [Z_{\psi\phi}] & [Z_{\psi\psi}] \end{bmatrix} \begin{bmatrix} [c_{s(-),k}]_k \\ [d_{s,k}]_{s,k} \end{bmatrix} = \begin{bmatrix} [0]_{k'} \\ [0]_{s',k'} \end{bmatrix} \quad (14a)$$

where,

$$Z_{\phi\phi}(k',k) = \langle \phi_{s(-),k'}(x), \hat{Z}\phi_{s(-),k}(x) \rangle = \sum_n^{NBTE} \langle \phi_{s(-),k'}(x), f_n^{TE}(x) \rangle z_n^{TE} \langle f_n^{TE}(x), \phi_{s(-),k}(x) \rangle + \sum_n^{NBTM} \langle \phi_{s(-),k'}(x), f_n^{TM}(x) \rangle z_n^{TM} \langle f_n^{TM}(x), \phi_{s(-),k}(x) \rangle \quad (14b)$$

$$Z_{\phi\psi}(k',k) = \langle \phi_{s(-),k'}(x), \hat{Z}\psi_{s,k}(x) \rangle = \sum_n^{NBTE} \langle \phi_{s(-),k'}(x), f_n^{TE}(x) \rangle z_n^{TE} \langle f_n^{TE}(x)), \psi_{s,k}(x) \rangle + \sum_n^{NBTM} \langle \phi_{s(-),k'}(x), f_n^{TM}(x) \rangle z_n^{TM} \langle f_n^{TM}(x)), \psi_{s,k}(x) \rangle \quad (14c)$$

$$Z_{\psi\phi}(k',k) = \langle \psi_{s',k'}(x), \hat{Z}\phi_{s(-),k}(x) \rangle = \sum_n^{NBTE} \langle \psi_{s',k'}(x), f_n^{TE}(x) \rangle z_n^{TE} \langle f_n^{TE}(x)), \phi_{s(-),k}(x) \rangle + \sum_n^{NBTM} \langle \psi_{s',k'}(x), f_n^{TM}(x) \rangle z_n^{TM} \langle f_n^{TM}(x)), \phi_{s(-),k}(x) \rangle \quad (14d)$$

$$Z_{\psi\psi}(k',k) = \langle \psi_{s',k'}(x), \hat{Z}\psi_{s,k}(x) \rangle = \sum_n^{NBTE} \langle \psi_{s',k'}(x), f_n^{TE}(x) \rangle z_n^{TE} \langle f_n^{TE}(x)), \psi_{s,k}(x) \rangle +$$

$\sum_n^{NBTM} \langle \psi_{s',k'}(x), f_n^{TM}(x)) \rangle z_n^{TM} \langle f_n^{TM}(x)), \psi_{s,k}(x) \rangle$ (14e)

It is easily shown that the admittances of TE and TM modes and the modal basis functions are expressed as function of the propagation constant β and the frequency f. The equation 16.a can be expressed as:

$$A(\omega, \beta)X = 0 \quad (15)$$

where $\omega = 2\pi f$.

The nontrivial solutions of the system of homogeneous equations Eq.(15) provide at a given frequency f , the constants of propagation of the modes guided by the structure.
The nontrivial solutions are obtained by cancelling the determinant of the matrix:

$$det[A(\beta)] = 0 \quad (16)$$

The Eq. (16) represents the characteristic equation of the system. Its resolution makes it possible to calculate β at a given frequency and thus the constant of propagation [23].

2.4 Optimization of the evaluation of matrix elements

Special attention must be given to the MR-GEC implementation. As wavelets are more complex, generates a wide variety of test functions and have larger supports for coarsest resolution than classical MOM functions, computing interactions between the elements of the matrix is much more time-consuming. Special computation rules must be defined, to speed up the algorithm while maintaining accuracy. Here we present the numerical implementation of the presented MR-GEC.

In the general structure of the matrix, we are led to the calculation of the following two terms as basis functions and test are real functions:

$$f^{\alpha}_{n,\phi_{s(-),k}} = \langle \phi_{s(-),k}(x), f_n^{\alpha}(x,y) \rangle; \ \forall k \in [0, 2^{s(-)} - 1]; \ \alpha \in \{TE, TM\} \quad (17a)$$

$$f^{\alpha}_{n,\psi_{s,k}} = \langle \psi_{s,k}(x), f_n^{\alpha x}(x,y) \rangle; \ \forall s \in [s(-), s(+)] \ \forall k \in [0, 2^s - 1]; \ \alpha \in \{TE, TM\} \quad (17b)$$

The corresponding terms described with equation (17a) are first computed with scaling function at a fine resolution level $(s(+) + 1)$.

$$f^{\alpha}_{n,\phi_{s(+)+1,k}} = \langle \phi_{s(+)+1,k}(x), f_n^{\alpha}(x) \rangle ; k \in [0, 2^{s(+)+1} - 1] \quad (18)$$

As we use wavelets on $[0,1]$, a linear mapping relation between the width of the microstrip line and $[0,1]$ is made.
The next step in our algorithm is to apply the pyramidal algorithm of Mallat from the fine resolution level (s (+) +1) to the coarse resolution level $s(-)$.This decomposition allows reducing the CPU time for the impedance matrix fill in.
The last step of the computation of the impedance matrix is a thresholding procedure. This is done in order to improve the compression rate of the entire generalized impedance matrix and then to reduce the memory storage and matrix solution time. Indeed, some of the elements, even in self-interaction sub-matrices, are small enough to be neglected. When the sub-matrix corresponds to the interaction of a metallization on itself, the first step of the thresholding approach is to look for the largest element of the impedance matrix Z. The other elements are thus compared to this reference value multiplied by a thresholding parameter δ.
The cancellation rule is defined as follows:

$$Z_{i,j} = 0 \ if \ |Z_{i,j}| < |Z_{max}| \times \delta \quad (19)$$

The compression rate is defined as follows:

$$TC(\%) = \frac{NBzero}{ns^2} \times 100 \quad (20)$$

3. Numerical results

Based on the procedure presented in the preceding sections, a set of MATLAB programs has been written to determine the dispersion curves and higher order modes of the shielded microstrip line by the MR-GEC.
There are two ways to represent the dispersion. The first is to provide the $\omega - \beta$ curves describing the variation of the propagation constant β as a function of frequency ω.
The second way is to represent the $\omega - \frac{\lambda_g}{\lambda_0}$ curves describing the variation of the normalized guide wavelength $\frac{\lambda_g}{\lambda_0}$ as a function of frequency ω.
To obtain these curves, it is necessary to calculate the value of the propagation constant β for each frequency and thereby deduce the guide wavelength λ_g and the effective permittivity of the dielectric ε_{eff} which is expressed by Eq. (21) [9]:

$$\varepsilon_{eff} = \left(\frac{\lambda_0}{\lambda_g}\right)^2 = \left(\frac{\beta}{k_0}\right)^2 \quad (23)$$

We used for this application the Haar wavelet as trial functions at one level of resolution $s(-) = s(+) = 2$. The matrix size is of the order of 8 X 8.
We expressed the basis functions on the interval [0,1] using a linear variable change, and then we calculated the scalar product defined by:

$$c_{3,k} = \left\langle f_n^{\alpha} \middle| \phi_{3,k} \right\rangle; k \in \left[0,2^3 - 1\right]; \alpha \in \{TE, TM\} \quad 24)$$

By these means the complete mode spectrum can be found with a comparatively small amount of computation. Indeed, convergence is reached only for 400 TE and TM modes. At convergence, the matrix is diagonally dominant and well-conditioned. Indeed, all relevant matrix elements are on the diagonal, it is a characteristic of the use of wavelets as test functions.
We are first interested to the study of the fundamental mode. A comparison was made with the results obtained in [9] for the same structure but studied by a spectral approach SDA based on the Green's functions.
Fig. 6 shows that there is good agreement between our results and those found in [9].

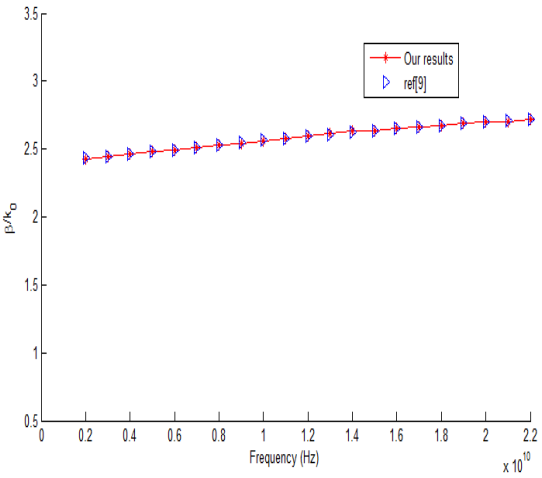

Fig.3 Normalized propagation constant $\frac{\beta}{k_0}$ versus frequency.

We then increasing frequency up to 30 GHz to better highlight the accuracy of our method. The same structure was also studied by Itoh and Mittra [6], [5], also in [25].
Fig.4 depicts the variation of the normalized guide wavelength of the fundamental mode for a frequency up to 30 GHz. We find good agreement with the results of references already cited.

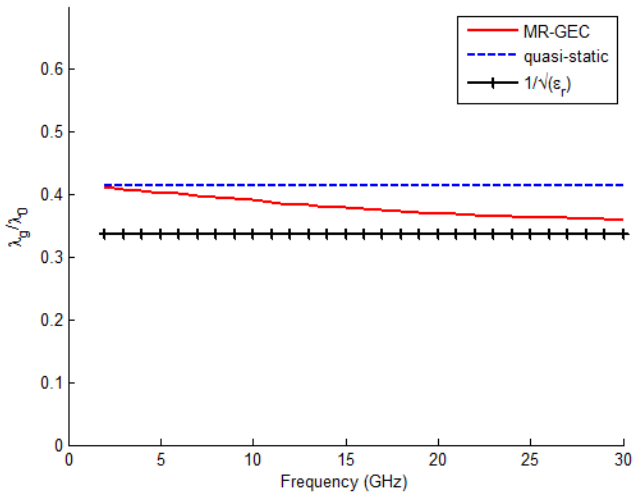

Fig.4 Normalized guide wavelength $\frac{\lambda_g}{\lambda_0}$ versus frequency.

We note that for a frequency below 5 GHz, our results coincide with those found by the quasi-static formula. We also note that the guide wavelength $\frac{\lambda_g}{\lambda_0}$ decreases with an increase in frequency and tend to the value $\frac{1}{\sqrt{\varepsilon_r}}$. This implies that the higher the frequency is, the more energy is propagated in the dielectric and below the metal strip [2].
In [26-2], an empirical formula is given by KOBAYASHI for computing the value of the effective dielectric permittivity.
To better approve the validity of our method, we compared the value of effective dielectric permittivity of the fundamental mode calculated by the MR-GEC with that calculated with the KOBAYASHI's formula for each frequency up to 30 GHz. Fig. 5 shows the results of this comparison and the resulting relative error does not exceed 0.55%.

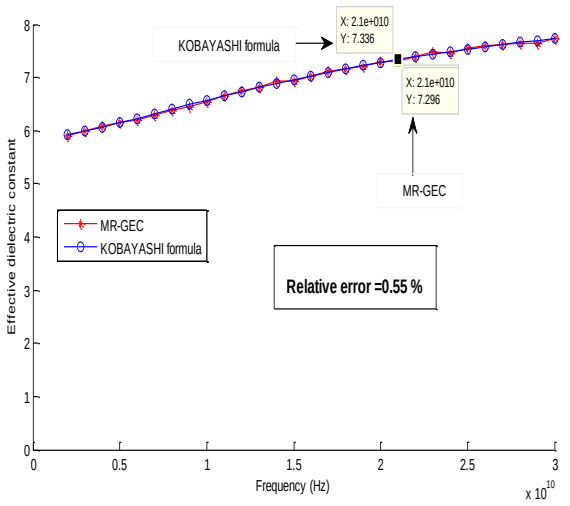

Fig.5 Effective dielectric constant ε_r versus frequency.

To get an idea on the number of roots that cancel the determinant, we can first calculate the cutoff frequencies of the shielded line. In this paper we will do this graphically. We set the value of the propagation constant β to zero, and then we calculate the determinant of the matrix for various frequencies. We note that the imaginary part of the determinant is always zero, while the real part is zero, but with a sudden change of sign in very specific frequencies, these frequencies are cutoff frequencies. The detection and calculation of a cutoff frequency begets the appearance of a new higher order mode.
Fig.6 shows an example of the graphical determination of cutoff frequencies in the range$[20\ GHz, 24\ GHz]$. We note the existence of three cutoff frequencies in this range: $Fc_1 = 21\ GHz, Fc_2 = 22.73$ GHz, et $Fc_3 = 23.98\ GHz$.

Typical plots of $det(A(\beta))$ versus frequency are shown in fig.7. It is observed that there can be more than one zero crossing of $\det(A)$, indicating the existence of higher order modes. As expected, the number of higher order propagating modes increases with increasing frequency [2].
Fig. 8 shows the dispersion diagram β-ω in the real plane neglecting the losses of the structure. We note that the solutions obtained are validated by comparison with those given by ROZZI in [19] and the fundamental mode appears to be unperturbed by the first higher order mode.

Fig. 8 shows the dispersion diagram $\beta - \omega$ characteristics of the first 8 modes computed for a choice of parameters identical to that used by Hornsby and Gopinath using a matrix size of the order of 100 X 100 [6] and by ROZZI in [19]. Their results are also exhibited on the same diagram to facilitate comparison. Although the present method uses only a 8 X 8 matrix, the results compare quite favorably with those already published.

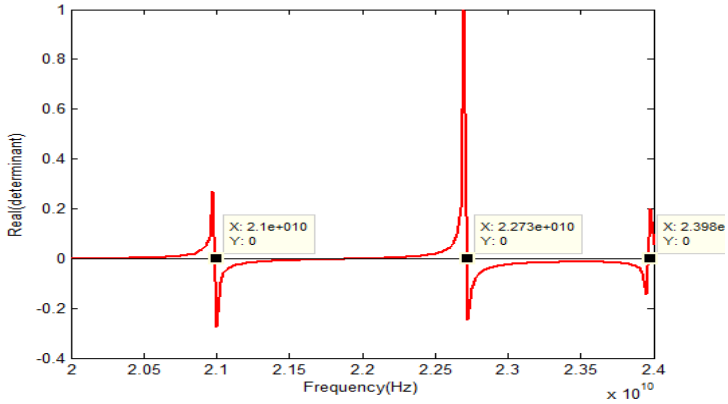

Fig. 6 Graphical compute of cutoff frequencies in the range$[20\ GHz, 24\ GHz]$.

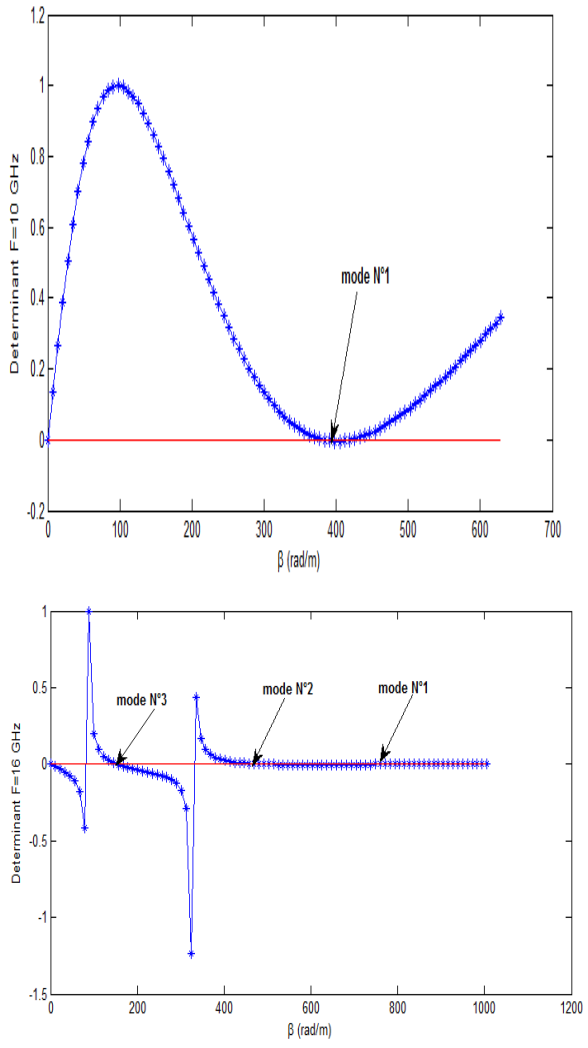

Fig. 7 Typical plots of $\det(A)$ versus β.

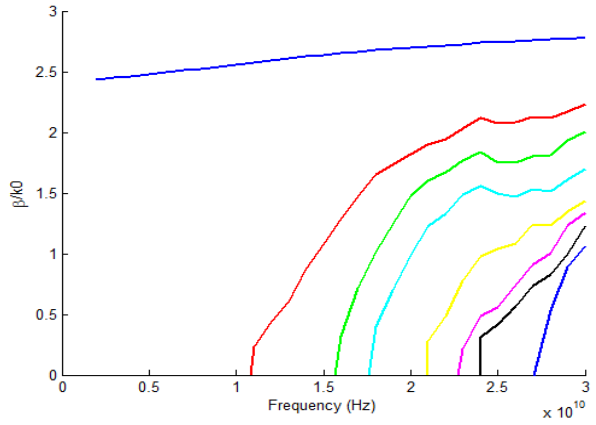

Fig. 8. Higher order modes of a shielded microstrip line.

Fig.9 shows the structure of impedance matrix for the studied structure for different values of threshold at the frequency $F = 16\,GHz$. We note that the higher the compression ratio is increasing the number of non-zero elements decreases and the matrix tends to be diagonally dominant.

In comparison with the exact value of the constant propagation of the dominant mode β obtained by using the original impedance matrix, the result computed by using the sparse matrix with until 68% nonzero entries demonstrates excellent accuracy. The error criterion of β is perhaps the most strict one. Indeed, with a compression ratio of 87%, which corresponds to 8 non-null elements of the matrix we find a value of the propagation constant β of the fundamental mode but with an error of 6%.

4. Conclusion

A new formulation of the moment method was presented in this paper to solve an electromagnetic problem. The conventional moment method was combined to the generalized equivalent circuit modeling to get an original and simple but rigorous formulation. This technique is based on the impedance operator and is applied to analyze the dispersion characteristics of a sielded microstrip line. A technique was presented to improve the performance of this method by introducing wavelet as trial functions. The application of the DWT allows the best case reduce the computation time.

The accuracy of the solution is demonstrated by comparing the present results with those derived by other authors using matrices with higher dimensions. Aside from the numerical efficiency of the method, the simplicity of the determinantal equation allows one to readily predict and extract higher order modal solutions for the wavenumber β from a study of the allure of the determinant of the impedance matrix A. The knowledge of the higher order solutions is important since they obviously affect the usefulness of the microstrip line at high frequencies.

The technique described in this paper works quite well with significant computational efficiency for planar microwave structures and could be extended to model multilayer structures.

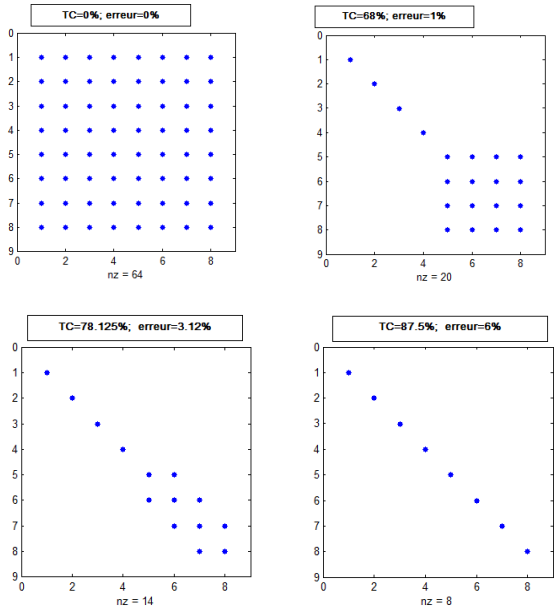

Fig. 9 Structure of impedance matrix after applying a threshold.

References

[1] R.E. Collin., "*Field Theory of Guided Waves*," 2nd ed., New York, 1987.

[2] K.G. Gupta, R. Garg and I.J. Bahal, "*Microstrip Lines and Slotlines*," Dedham, MA:Artech House, Inc., 1979.

[3] M. L. Tounsi, C.E. Yagoub, and B. Haraoubia, "New design formulas for microstrip transmission lines using high-dielectric substrate," *International Journal for Computation and Mathematics*, Vol.24, pp.15 – 34, 2005.

[4] T. C.Edwards, "Foundations for Microstrip circuits desing," New York: John Wiley & Sons, 1981.

[5] R. Mittra, and T.Itoh, "A new technique for the analysis of the dispersion characteristics of microstrip lines," IEEE Transactions on Microwave Theory and Techniques, Vol. Mtt19, no. 1, January 1971.

[6] T. Itoh, and R. Mittra, "Spectral-domain approach for calculating the dispersion characteristics of microstrip lines," IEEE Transactions on Microwave Theory and Techniques, July 1973.

[7] T. Itoh, and R. Mittra, "A technique for computing dispersion characteristics of shielded microstrip lines," ibid., Vol . MTT-22, pp. 896-898, Oct. 1974.
[8] T. Itoh, "Spectral domain immittance approach for dispersion characteristics of generalized printed transmission lines," ibid., Vol. MTT-28, pp. 733-736, July 1980.
[9] S. Redadaa, and M. Benslama, "Analysis of Dispersion Characteristics of Microstrip Lines", SETIT 2005.
[10] H. Baudrand, "Tridimensional methods in monolithic microwave integrated circuits," *SMBO Brazilian Symposium NATAL*, pp. 183-192, 27-29 July 1988.
[11] H. Baudrand, "Representation by equivalent circuit of the integral methods in microwave passive elements," 20th EMC, Budapest 10-14 Sep. 1990.
[12] H. Aubert and H. Baudrand, "L'Electromagnétisme par les schémas équivalents, " Cepaduès Editions 2003.
[13] T. Aguili, "Modélisation des composantes SFH planaires par la méthode des circuits équivalents généralisées," Thesis Manuscript, National Engineering School of Tunis, Tunisia, 2000.
[14] B. Z. Steinberg and Y. Leviatan, "On the use of wavelet expansions in the method of moments," IEEE *Trans. Antennas and Propag.* Vol 41 N°5, pp. 610-619, 1993.
[15] X. Zhu, T. Sogaru and L. Carin, "Three-dimensional biorthogonal multiresolution time-domain method and its application to electromagnetic scattering problems," IEEE *Trans. Antennas and Propag.* Vol 51, N°5, pp. 1085-1092, May 2003.
[16] Daubechies, I., "Ten Lectures on Wavelets", SIAM, Philadelphia, 1992.
[17] Chui, C. K., "An Introduction to Wavelets," Academic Press, 1991.
[18] Chui, C. K., "Wavelets — A Tutorial in Theory and Applications, "Academic Press, 1992.
[19] C.J. Railton and T. Rozzi, "Complex modes in boxed microstrip," IEEE Transactions on Microwave Theory and Techniques, vol. *36*, no. 5, May 1988.
[20] G. Wang, "On the Utilization of Periodic Wavelet Expansions in the Moment Methods," *IEEE transactions on microwave theory and techniques*, Vol. 43, no. 10, Oct. 1995.
[21] G. Wang, "Application of Wavelets on the Interval to the Analysis of Thin-Wire Antennas and Scatterers," *IEEE transactions on antennas and propagation*, Vol. 45, no. 5, May 1997.
[22] F. J. Narcowich, "First Course In Wavelets With Fourier Analysis," Wiley; Oct. 2009.
[23] T. Itoh, "Spectral domain immittance approach for dispersion characteristics of generalized printed transmission lines," ibid., vol. MTT-28, pp. 733-736, July 1980.
[24] M. K. Krage and G. I. Haddad, "Frequency-dependent characteristics of microstrip transmission lines," ibid., Vol. MTT-20, pp. 678-688, Oct. 1972.
[25] P. Xun, Q. Wang, F. Wang, S. Yu, and S. Liu, " The dispersion characteristics of shielded microstrip lines on magnetizes ferrite and anisotropic dielectric substrates", International Journal of Infrared and Millimeter Waves, vol. 11, No. 12, 1990.
[26] M. Kobayashi, "A dispersion formula satisfying recent Requirements in Microstrip Cad," IEEE Transactions on Microwave Theory and Techniques, vol. 36, no. 8, August 1988.
[27] Markuwitz, N., "*Waveguide Handbook*, "Wiley-Interscience, New York, 1986.
[28] H. Baudrand, "Introduction au calcul de circuits microondes, " INPT, ENSEEIHT, Edition 1993.

N. Oueslati received her Ing. degree in Telecommunications and her Master degree in Communication Systems from the Ecole Nationale d'Ingénieurs de Tunis (ENIT), Tunisia. She is currently working towards her Ph.D. degree in telecommunications at Communication Systems Laboratory, ENIT, Tunisia. Her current research interest includes passive and active microwave structures.

T. Aguili is working as Professor at the Ecole Nationale d'Ingénieurs de Tunis (ENIT), Tunisia. He received his Dip.Ing in Electrical Engineering, and Ph.D. in Telecommunications from INSA France. His research interests include passive and active microwave structures and optical communications.